

多重孪晶钯颗粒的可见光简易合成及对乙醇的电催化氧化

谭德新¹ 王艳丽^{*,2,3} 甘 颖¹ 胡 伟²

(¹ 安徽理工大学化学工程学院, 淮南 232001)

(² 安徽理工大学材料科学与工程学院, 淮南 232001)

(³ 安徽理工大学博士后科研流动站, 淮南 232001)

摘要: 以氯化钯(PdCl_2)为金属前驱体,乙醇为还原剂,聚乙烯吡咯烷酮(PVP)为稳定剂和导向剂,利用普通市售节能灯产生的光热作用,辅助制备多重孪晶钯纳米颗粒。用 HRTEM、FFT、PXRD、XPS、UV-Vis 和 FT-IR 等技术对产品的形貌、晶体结构、光学性质和稳定性进行了表征,并通过循环伏安法研究了多重孪晶 Pd 修饰玻碳电极对乙醇的电催化氧化活性。结果表明,多重孪晶钯结构的形成依赖于光和热的协同作用。该材料的表面等离子共振吸收峰在可见光区域,对乙醇有较好的电催化活性和抗中毒能力。

关键词: 钯; 多重孪晶颗粒; 可见光; 乙醇; 电催化氧化

中图分类号: O614.82·3 文献标识码: A 文章编号: 1001-4861(2016)03-0475-08

DOI: 10.11862/CJIC.2016.05

Palladium Multiply Twinned Particles: a Facile Visible-Light-Assisted Synthesis and Electrooxidation of Ethanol

TAN De-Xin¹ WANG Yan-Li^{*,2,3} GAN Ying¹ HU Wei²

(¹School of Chemical Engineering, Anhui University of Science and Technology, Huainan, Anhui 232001, China)

(²School of Materials Science and Engineering, Anhui University of Science and Technology, Huainan, Anhui 232001, China)

(³Post-doctoral Research Station, Anhui University of Science and Technology, Huainan, Anhui 232001, China)

Abstract: Using palladium chloride (PdCl_2) as the palladium precursor, ethanol as reducing agent and poly (vinyl pyrrolidone) (PVP) as a stabilizer and guiding agent, palladium (Pd) multiply twinned particles (MTPs) were synthesized via photothermally assisted solution approach with visible light from a commercial energy-saving lamp as light source. The morphologies, crystal structure, optical properties and the stability of Pd MTPs were characterized by high resolution transmission electron microscopy (HRTEM), fast Fourier transformation (FFT), powder X-ray diffraction (PXRD), X-ray photoelectron spectroscopy (XPS), UV-Visible spectroscopy and Fourier transform infrared (FT-IR) spectroscopy, respectively. The electrocatalytic properties of the Pd MTPs modified glassy carbon electrode for ethanol oxidation were investigated by cyclic voltammetry. The results showed that the formation of Pd MTPs depends on the coordination interaction of light and thermal effects. Surface plasmon resonance (SPR) peak of Pd MTPs is located at the visible region. This material exhibits remarkable electrocatalytic activity and anti-poisoning faculty for the ethanol oxidation.

Keywords: palladium; multiply twinned particles; visible light; ethanol; electrooxidation

收稿日期: 2015-06-12。收修改稿日期: 2016-01-06。

国家自然科学基金(No.51303005)、安徽省教育厅重点基金(No.KJ2013A087, KJ2013A095)和安徽省博士后基金(No.2015B063)资助项目。

*通信联系人。E-mail: ylwang1998@163.com

0 Introduction

Noble metal nanoparticles are very important for potential applications in several technological fields, such as electrochemistry, photonics, magnetic storage, sensing, plasmonics and catalysis^[1-2]. As a noble metal, Pd nanoparticles have been widely used as catalysts for alkene hydrogenation^[3], alcohol oxidation^[4], trichloroethene hydrodechlorination^[5], Suzuki-Miyaura^[6], Heck^[7], and Stille coupling reactions^[8]. Moreover, another important property of Pd nanoparticles is their surface plasmon resonance (SPR) features, which can lead to applications in colorimetric sensing, plasmonic waveguiding, enhancement of electromagnetic fields and light transmission, and optical sensing of hydrogen^[9]. The properties of nanomaterials are determined by their shape, size, composition, crystallinity, and structure^[10-12]. Pd is a face-centered cubic (fcc) noble metal. It may take three different shapes when fast nucleation and growth are involved: truncated cubes or octahedra, decahedra, and icosahedra^[13]. The truncated cubes or octahedra are single crystals, whereas both decahedra and icosahedra are multiply twinned particles (MTPs). In 1966, Au MTPs were synthesized firstly by deposition of Au on NaCl surface in ultrahigh vacuum^[14]. Since that, owing to MTPs with unique microstructures (shape with multiple facets) and formation mechanisms, several metals MTPs have been obtained and their potential application in catalysis, gas sensors, and electronics have been investigated^[15-20]. However, MTPs have never been the major product of typical solution-phase syntheses. For example, only 10% decahedra could be obtained by fast reduction of $\text{Na}_2[\text{PdCl}_4]$ using ethylene glycol, and the major product (90%) was truncated cubes or octahedral^[21]. Therefore, it still remains a grand challenge to synthesize Pd MTPs in relatively high yields.

Recently, photochemical and irradiation synthesis has been proven to be a promising route for the preparation of various nanomaterials^[22]. Current photochemical methods focus mainly on the use of high-energy radiation, such as UV light or γ -irradiation^[23-24]. It is therefore important to design a safer, cheaper,

and more facile light-assisted method to nanomaterials. Retna Raj^[25] has presented a facile photochemical route for the synthesis of triangular Ag nanoplates using sunlamp, and the result demonstrated that light can induce shape transformation of Ag nanoplates.

Based on the fact that Ag nanoplates could be obtained using sunlamp, we have presented a novel visible-light-assisted method to synthesize Pd MTPs in relatively high yields (a proportion of 99%). In this paper, using palladium chloride (PdCl_2) as the Pd precursor, ethanol as reducing agent and poly (vinyl pyrrolidone) (PVP) as a stabilizer and guiding agent, Pd MTPs were synthesized via a commercial energy-saving lamp as light source, and the influence of light and heat on the morphology of products have been also investigated. The study of UV-visible spectroscopy and cyclic voltammetry (CV) reveals that the as-prepared Pd MTPs exhibit good optical and electrochemical properties.

1 Experimental

1.1 Materials

PdCl_2 and ethanol were obtained from Nanjing Chemical Reagent No.1 Factory. PVP was purchased from Sinopharm Chemical Reagent Co. Ltd. All other chemicals were analytical grade and used as received. All the aqueous solutions were prepared with twice-distilled water.

1.2 Preparation of the suspensions of Pd MTPs

In a typical synthesis, a solution of $17.5 \mu\text{mol}$ PdCl_2 and $1.69 \mu\text{mol}$ PVP were mixed with 4 mL of ethanol and 20 mL of deionized water in a 0.10 L glass vessel. The mixture was dispersed to form a homogeneous solution by constant strong stirring for 2 h. Then, the mixture was irradiated for 64 h with visible light from the 11-Watt energy-saving lamp at a distance of 5 cm. The brown suspensions was precipitated by acetone and washed with ethanol three times to remove excess PdCl_2 and surfactants. The final brown product could be easily redispersed in polar solvents such as ethanol and water to yield a clear homogeneous solution.

1.3 Characterization

The high resolution transmission electron microscopy (HRTEM) images and fast Fourier transformation (FFT) were performed with a Tecnai G2 F20 instrument operated at 200 kV. The powder X-ray diffraction (PXRD) pattern was recorded on a XD-3 type X-ray diffractometer employing Cu $K\alpha$ radiation ($\lambda=0.154$ nm, $V=36$ kV, $A=30$ mA). X-ray photoelectron spectroscopy (XPS) was performed on an ESCALAB 250 instrument. The binding energies obtained in the XPS spectral analysis were corrected for specimen charging by referencing the C1s to 284.6 eV. The UV-Visible spectroscopy of the prepared suspensions was obtained by an UV-Visible spectro-photometer (UV-2600) from Shimadzu with quartz cuvettes. The Fourier transform infrared (FT-IR) spectroscopy was obtained using a Nicolet spectrometer model 380 FT-IR on KBr pellet of the samples.

1.4 Electrochemistry tests

Electrochemical measurements were performed with a CHI 660E electrochemical workstation (CH Instruments, Chenhua Co., Shanghai, China) at room temperature, and conducted on a conventional three-electrode cell, which includes a platinum wire as counter electrode, a saturated calomel electrode (SCE) as reference electrode and the Pd-modified glassy carbon electrode (GCE, 3 mm in diameter) as working electrode. In all electrochemical measurements, the current densities were normalized to the geometric surface area of the GCE.

For the preparation of the Pd nanomaterials modified electrode, 5 μL of a suspension containing Pd nanomaterials was dropped on the clean electrode surface and dried in air. Next, the Nafion film was prepared by dropping 3 μL of a Nafion solution (0.1%, w/w) onto the electrode and allowed the solvent to evaporate at room temperature. Cyclic voltammogram (CV) of the Pd nanomaterials modified electrode were recorded in a 1 mol $\cdot\text{L}^{-1}$ KOH solution containing 1 mol $\cdot\text{L}^{-1}$ ethanol. The solutions were deaerated thoroughly for at least 30 min with pure nitrogen gas and kept under a positive pressure of this gas during the experiments.

2 Results and discussion

2.1 Structural analysis of Pd MTPs

In this work, the experimental setup is shown in Fig.1a. The suspensions changed its color from yellow to brown after it had been irradiated for 64 h. The nanoobjects observed are formed of Pd MTPs (Fig.1b). These MTPs were reported for Au and Ag to exhibit generally five-fold symmetry^[26-28]. In the present case, a relatively high proportion (99%) of Pd MTPs with a mean dimension of (20 ± 1) nm was observed (Fig.1b). HRTEM image (Fig.1c) showed Pd MTPs were covered only by (111) planes. The FFT of the image at higher magnification revealed two main diffraction rings. The reciprocal distances found $d_1=0.225$ nm and $d_2=0.199$ nm correspond to the (111) and (200) plane lattices of cubic Pd (Fig.1d). The formation of MTPs has been explained by several mechanisms, such as errors during the growth leading to twins, intrinsic equilibrium structures of the lower energy at smaller size, layer by layer growth around the 5-fold symmetry axes, and a phase transformation to an orthorhombic or rhombic form. To date, most of the evidence directs one to the mechanism of intrinsic equilibrium^[28-29].

The phase purity and high crystallinity of Pd MTPs was also supported by powder X-ray diffraction (PXRD). Five characteristic peaks of Pd at $2\theta=40.06^\circ$, 46.56° , 68.08° , 82.06° , 86.60° , corresponding to the (111), (200), (220), (311) and (222) lattice planes, are observed. All the diffraction peaks can be well-indexed to fcc Pd according to the JCPDS card No.05-0681, indicating that the as-prepared Pd MTPs have a high purity and high crystallinity. The lattice parameters of Pd MTPs were, $a=b=c=0.3894$ nm and $\alpha=\beta=\gamma=90^\circ$ calculated by PXRD analysis. It was worth noting that the ratio between the intensities of (111) and (200) peaks was much higher than the index value (2.86 vs 2.38), indicating that the top and bottom faces of each nanoparticle were bounded by 111 planes. These nanoparticles were more or less oriented parallel to the supporting substrate, resulting in a stronger (111) diffraction peak than that of a

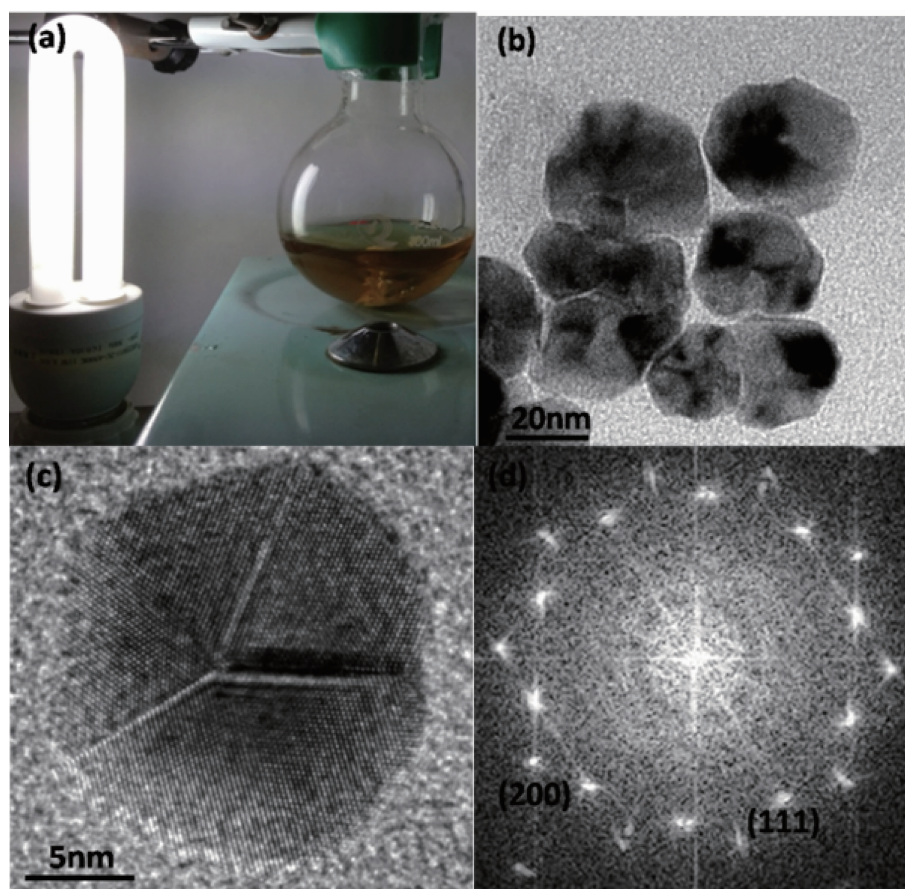


Fig.1 (a) An experimental setup image of the visible-light-assisted method; TEM (b) and HRTEM (c) of Pd MTPs and its corresponding FFT (d)

conventional powder sample. According to the Scherrers equation, the reflecting peaks at $2\theta=40.06^\circ$ and 68.08° were chosen to calculate the average diameter, the average size of Pd MTPs was about 20 nm, which was excellently consistent with the observation by HRTEM.

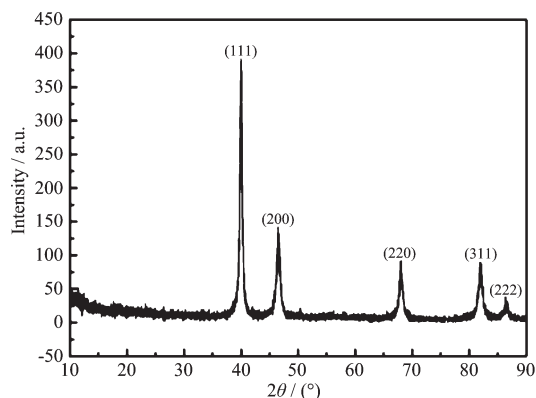


Fig.2 PXRD pattern of Pd MTPs

XPS was carried out to investigate the chemical states of the as-prepared products obtained in systems

(see Fig.3). The sample appeared as a spin-orbit doublet at 340.6 eV ($3d_{3/2}$) and 335.55 eV ($3d_{5/2}$), which was in agreement with the reported value in the literature^[30]. Consequently, on the basis of the results of PXRD and XPS measurements, the as-synthesized products could be determined as Pd (0). Additionally, Pd(0) content was 4.31% by XPS analysis.

The optical properties of the Pd MTPs have been

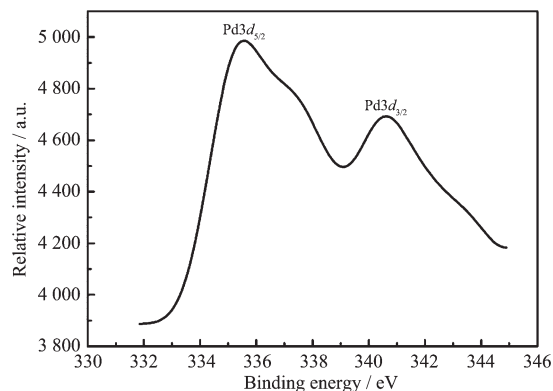


Fig.3 XPS spectrum of Pd MTPs

investigated using UV-Visible spectroscopy. SPR peak of small Pd nanoparticles (typically <10 nm in size) have no resonance between 300 and 1 500 nm, which gives them an uninteresting black color and makes their SPR characteristics much more difficult to probe due to the strong absorption of light at these wavelengths by glass and most solvents^[31]. Fig.4 shows UV-Visible spectra taken from aqueous suspensions of Pd MTPs. Note that the surfaces of as-prepared Pd particles are usually covered by PVP, which has an absorption peak at 212 nm^[21,32-33]. The SPR peak of Pd MTPs could be located at 304 nm, which shifted to above 300 nm. Considering narrower particle size distribution of MTPs, the SPR peak over the entire spectrum became very sharp. The exceptional SPR features of those Pd MTPs should make them potentially useful as nanoscale photothermal heating elements^[34].

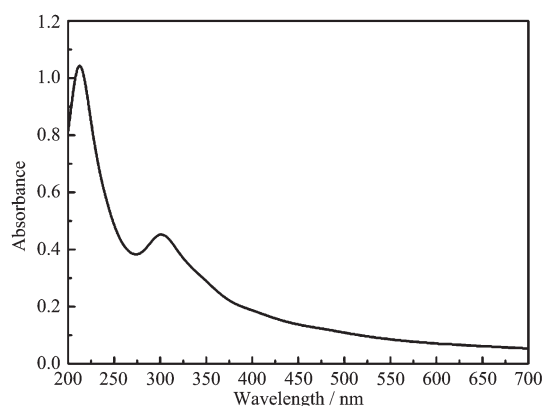


Fig.4 UV-Visible spectroscopy of Pd MTPs

The stability of nanoparticles suspensions was studied through the direct observation method reported by Cárdenas-Triviño^[35]. It was clearly found that the obtained Pd MTPs suspensions absorbed visible light strongly and thus had a dark brown color. Furthermore, there no segregation between the solvent and the black Pd particles was observed for more than 10 months. The stabilization of Pd MTPs has been also investigated using the FT-IR spectroscopy. The obtained spectrum of Pd MTPs is shown in Fig.5. The absorption band appearing at 1 643 cm^{-1} was assigned to the stretching vibration mode of the C=O (PVP), in the nanoparticle suspensions. During the preparation of PVP/sodium montmorillonite nanocomposite, Koo^[36] attributed the shift of the C=O (PVP) absorption towards low frequencies to the interaction between C=O (PVP) and the silicate surface. In this study, the shift of the PVP carbonyl position in PVP-Pd powder, compared to the C=O (PVP) adsorption position at 1 654 cm^{-1} and to the C=O (PVP-Pd) position at 1 643 cm^{-1} , is essentially due to the interaction between C=O (PVP) and Pd nanoparticles surface. This result is in good agreement with those reported in earlier studies^[37-38], where it has been concluded that the PVP can protect the metal nanoparticles via the carbonyl group.

To determine the role of light and thermal effects in the formation of these Pd MTPs, we performed several control experiments in which the amount of

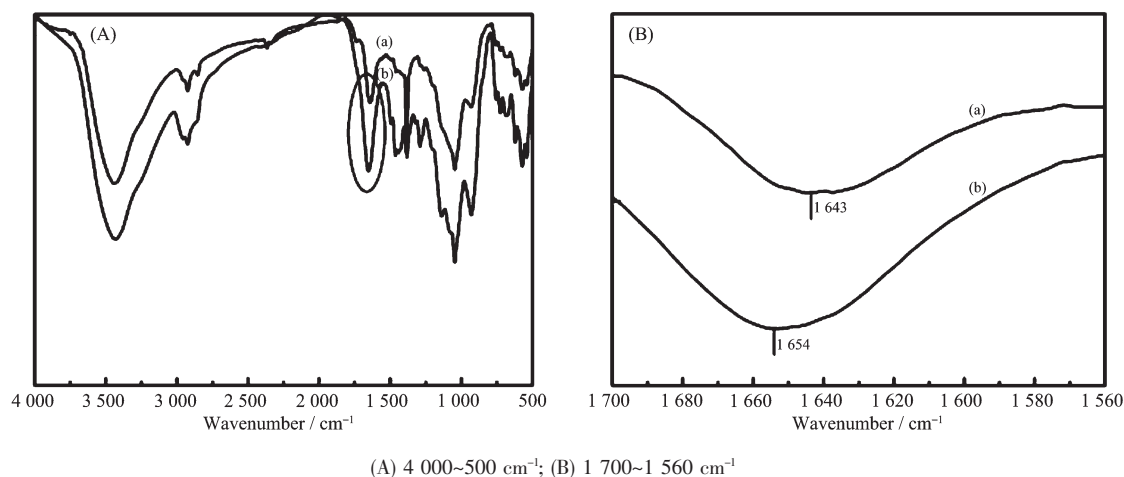
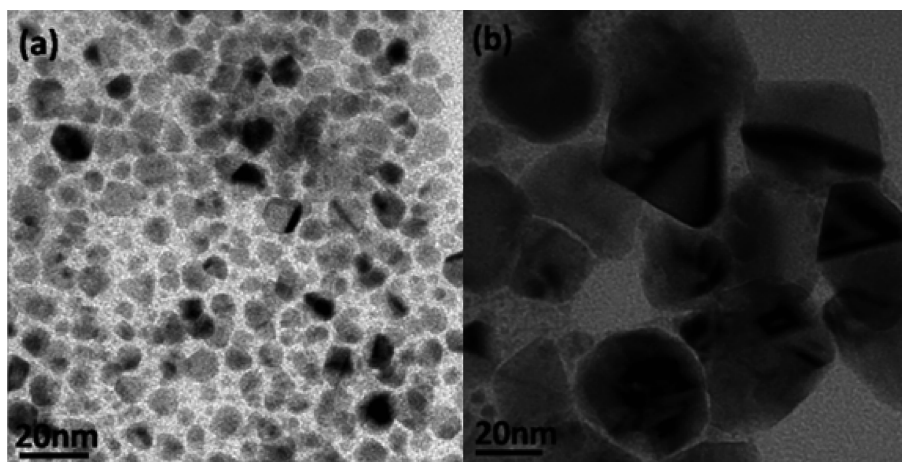


Fig.5 FTIR spectra of Irradiated sample (PVP-Pd) (a) and Pure PVP (b)



Reaction mixture: (a) heated at 22 °C by a conventional heating technique; (b) irradiated with the 11-Watt ultraviolet lamp

Fig.6 TEM images of Pd nanoparticles formed under different reaction conditions

the reagents was controlled to be identical to that of Pd MTPs. In this method, we found that the solution phase temperature was about (21 ± 1) °C when an 11-Watt energy-saving lamp was used. Therefore, to clarify the role of the light, a conventional heating method was applied to the solution systems. We found that ultrafine quasi-spherical Pd nanoparticles (Fig.6a) with an average size of (9 ± 1) nm were obtained in the dark chamber when the solution with same amounts of PdCl_2 and PVP and the temperature was 22 °C. In addition, we found that a relatively high proportion (71%) of stacked Pd nanoplates (Fig.6b) with a mean dimension of 26 nm were obtained when the reaction mixture was irradiated with the 11-Watt ultraviolet lamp, which confirms the critical role of thermal effects in controlling the morphology. Thus, our visible-light-assisted method is obviously different from both the conventional heating method and UV irradiation method. We suppose that photoirradiation and thermal effects contribute simultaneously to the controlled synthesis of Pd MTPs.

2.2 Catalytic activity

As a matter of fact, it has been established that

Pd has no activity for alcohol electrooxidation in acidic media. In contrast, Pd has been demonstrated to be very active and even more efficient than Pt for ethanol oxidation in alkaline medium^[39]. In this study, the electrode, which were modified by Pd MTPs, was labeled as Pd/GCE (I); The electrode, which were modified by ultrafine quasi-spherical Pd nanoparticles, were labeled as Pd/GCE(II); The electrode, which were modified by stacked Pd nanoplates, were labeled as Pd/GCE (III); Fig.6 displays the comparison of CV curves of bare GCE, Pd/GCE(I), Pd/GCE(II) and Pd/GCE (III). The main characteristics which can be measured from such voltammograms include: E_{onset} is the faradaic current onset potential; E_f is the forward peak potential; E_b is the backward peak potential; j_f is the forward current density; j_b is the backward current density. And these values relative to ethanol oxidation are given in Table 1. This set of parameters in Table 1 indicated that the oxidation of ethanol was more favorable with Pd MTPs.

Well-defined CV features are observed in Fig.7 on all Pd/GCE, except for bare GCE. The ethanol electrooxidation shows completely irreversible in

Table 1 Cyclic voltammetry parameters for ethanol oxidation on different electrodes in $1 \text{ mol} \cdot \text{L}^{-1} \text{ KOH} + 1 \text{ mol} \cdot \text{L}^{-1} \text{ C}_2\text{H}_5\text{OH}$

Electrode	$E_{\text{onset}} / \text{mV}$	E_f / mV	E_b / mV	$j_f / (\text{mA} \cdot \text{cm}^{-2})$	$j_b / (\text{mA} \cdot \text{cm}^{-2})$	j_f / j_b
Pd/GCE(I)	-850	-254	-499	14.14	1.48	9.55
Pd/GCE(II)	-711	-219	-517	8.14	1.40	5.81
Pd/GCE(III)	-686	-253	-510	5.81	1.73	3.35

alkaline medium and has been characterized by two well defined anodic current peaks: one in the forward (*i.e.* anodic condition) and the other one in the reverse scan (*i.e.* cathodic condition). In the forward scan, the oxidation peak is corresponding to the oxidation of freshly chemisorbed species coming from ethanol adsorption. The oxidation peak in the reverse scan is primarily associated with the removal of carbonaceous species not completely oxidized in the forward scan, rather than caused by oxidation of freshly chemisorbed species^[40]. So the ratio of forward current density to backward current density, j_f/j_b , could be used to describe the catalyst tolerance to carbonaceous species accumulation^[41-42]. Obviously, among these Pd nanomaterials modified electrode, the j_f value ($14.14 \text{ mA} \cdot \text{cm}^{-2}$) and the j_f/j_b value (9.55) of Pd/GCE(I) is the biggest, revealing better electrocatalytic activity and poison tolerance of Pd MTPs as a catalyst. By comparison of micro-morphology of these Pd nanomaterials, we suspect that high proportion of diffraction planes exposed on Pd MTPs is considered the fundamental cause for the activity increase of ethanol electro-oxidation.

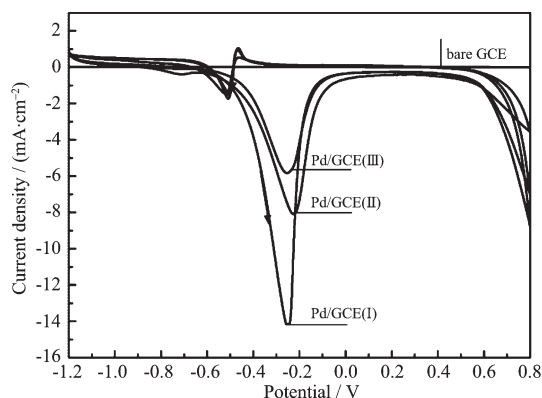


Fig.7 Cyclic voltammograms for bare GCE, Pd/GCE(I), Pd/GCE(II) and Pd/GCE(III) in $1 \text{ mol} \cdot \text{L}^{-1} \text{ C}_2\text{H}_5\text{OH} + 1 \text{ mol} \cdot \text{L}^{-1} \text{ KOH}$

3 Conclusions

In summary, a facile visible-light-assisted method has been developed for the synthesis of Pd MTPs. Both light and thermal effects play significant roles in this visible-light-assisted method. These Pd MTPs play good optical properties and their SPR peak is

located above 300 nm. In addition, these Pd MTPs exhibit the remarkable electrochemical properties for ethanol oxidation. Although detailed investigations concerning the exact photothermal role and the growth mechanism are still in progress, this novel method can be potentially extended to fabricate Pd MTPs materials with interesting morphologies. Furthermore, it is worth pointing out that these Pd MTPs might find use as catalysts, photothermal heating elements, absorption contrast agents, and chemically specific optical sensors.

References:

- [1] Imura Y, Tsujimoto K, Morita C, et al. *Langmuir*, **2014**,**30**: 5026-5030
- [2] Marcilla R, Curri M L, Cozzoli P D, et al. *Small*, **2006**,**2**:507-512
- [3] Nikoshvili L, Shimanskaya E, Bykov A, et al. *Catal. Today*, **2015**,**241**:179-188
- [4] Yang Z W, Zhao X, Li T J, et al. *Catal. Commun.*, **2015**,**65**: 34-40
- [5] Pretzer L, Song H, Fang Y, et al. *J. Catal.*, **2013**,**298**:206-217
- [6] Wen M, Takakura S, Ku K F, et al. *Catal. Today*, **2015**,**242**: 381-385
- [7] Wang P, Zhang G, Jiao H, et al. *Appl. Catal. A*, **2015**,**489**: 188-192
- [8] Saha D, Sen R, Maity T, et al. *Langmuir*, **2013**,**29**:3140-3151
- [9] Tobiška P, Hugon O, Trouillet A, et al. *Sens. Actuators B-Chem.*, **2001**,**74**:168-172
- [10] Madhumitha G, Roopan S M. *J. Nanomater.*, **2013**,**169**:1-12
- [11] Roopan S M, Khan F N, Mandal B K. *Tetrahedron Lett.*, **2010**,**51**:2309-2311
- [12] Jackson J B, Halas N J. *J. Phys. Chem. B*, **2001**,**105**:2743-2746
- [13] Baletto F, Ferrando R, Fortunelli A, et al. *J. Chem. Phys.*, **2002**,**116**:3856-3863
- [14] Ino S. *J. Phys. Soc. Jpn.*, **1966**,**21**:346-362
- [15] Huang P, Dai G Q, Wang F, et al. *Appl. Phys. Lett.*, **2009**, **95**:203101-203103
- [16] Santiago U, Velázquez-Salazar J J, Sanchez J E, et al. *Surf. Sci.*, **2016**,**644**:80-85
- [17] Zhu Y T, Liao X Z, Wu X L. *Prog. Mater. Sci.*, **2012**,**57**:1-62

- [18]Shao Y F, Wang S Q. *Ser. Mater.*, **2010**,**62**:419-422
- [19]Zhang Q, Xie J, Yang J, et al. *ACS Nano*, **2009**,**3**:139-148
- [20]Liang G F, He L M, Cheng H Y. *J. Catal.*, **2015**,**325**:79-86
- [21]Xiong Y, Chen J, Wiley B, et al. *J. Am. Chem. Soc.*, **2005**,
127:7332-7333
- [22]Zhang B, Dai W, Ye X C, et al. *Angew. Chem. Int. Ed.*,
2006,**45**:2571-2574
- [23]Navaladian S, Viswanathan B, Viswanath R P. *Nanoscale Res. Lett.*, **2009**,**4**:181-186
- [24]Rojas J V, Castano C H. *Radiat. Phys. Chem.*, **2012**,**81**:16-21
- [25]Bera R K, Raj C R. *J. Photochem. Photobiol. A-Chem.*, **2013**,**270**:1-6
- [26]Chen H, Gao Y, Zhang H, et al. *J. Phys. Chem. B*, **2004**,
108:12038-12043
- [27]Gai P L, Harmer M. *Nano Lett.*, **2002**,**2**:771-774
- [28]Zhang S H, Jiang Z Y, Xie Z X, et al. *J. Phys. Chem. B*,
2005,**109**:9416-9421
- [29]Marks L D. *Rep. Prog. Phys.*, **1994**,**57**:603-649
- [30]Siril P F, Ramos L, Beaunier P, et al. *Chem. Mater.*, **2009**,
21:5170-5175
- [31]Xiong Y J, McLellan J M, Chen J Y, et al. *J. Am. Chem. Soc.*, **2005**,**127**:17118-17127
- [32]Xiong Y J, Chen J Y, Wiley B, et al. *Nano Lett.*, **2005**,**5**:
1237-1242
- [33]Chen J Y, Herricks T, Geissler M, et al. *J. Am. Chem. Soc.*,
2004,**126**:10854-10855
- [34]Hirsch L R, Stafford R J, Bankson J A, et al. *Proc. Natl. Acad. Sci. U.S.A.*, **2003**,**100**:3549-3554
- [35]Cárdenas-Triviño G, Segura R A, Reyes-Gasga J. *Colloid Polym. Sci.*, **2004**,**282**:1206-1212
- [36]Koo C M, Ham H T, Choi M H, et al. *Polymer*, **2003**,**44**:
681-689
- [37]Nemamcha A, Rehspringer J L, Khatmi D. *J. Phys. Chem. B*, **2006**,**110**:383-387
- [38]Yonezawa T, Imamura K, Kimizuka N. *Langmuir*, **2001**,**17**:
4701-4703
- [39]Liu J, Ye J, Xu C, et al. *Electrochem. Commun.*, **2007**,**9**:
2334-2339
- [40]Singh R N, Singh A. *Anindita. Carbon*, **2009**,**47**:271-278
- [41]Huang T, Jiang R R, Zhang D, et al. *J Solid State Electrochem.*, **2010**,**14**:101-107
- [42]Zhao G Y, Xu C L, Guo D J, et al. *J. Power Sources*, **2006**,
162:492-496